constitutes the limit provided in the numerical program. This situation is a consequence of the accuracy that may be obtained from the shape of the maxima in the presence of losses.

In the case of line 10, the losses differ by 13 percent, due the aforestated problem caused by the nonshorted end of the sample; in fact, the apparent losses obtained are greater than the correct one. In the remaining cases the differences are less than 4 percent.

V. CONCLUSIONS

A method for measuring the complex electrical permittivity at microwave frequencies has been developed. It consists of the experimental determination and subsequent fitting of the field pattern existing in a sample placed inside a slotted waveguide closed by a short circuit.

The estimated precision of this method is about 0.1 percent for the real part of the permittivity and a few percent for the losses.

Owing to the fact that the oscillator in the experimental setup works under constant load conditions, it is not necessary to achieve a good isolation between the oscillator and the load, this being a problem which is present in the greatest part of waveguide measurement methods.

In comparison with the Roberts–von Hippel method, the proposed one offers the advantage that the possibility of false results is eliminated. On the other hand, it has been found that any irregularity existing in the nonshorted end of the sample will generate new modes which, even being evanescent, will produce an apparent increase in the loses of the material, if the measurements are carried out in the medium preceding the sample, as they are in the previously mentioned method. This problem may be eliminated with the proposed method, carrying out the measurements far enough from the end of the sample, at least when measuring materials with sufficiently low permittivities, to prevent new propagating modes.

REFERENCES

[1] S. Roberts and A. R. von Hippel, "A new method for measuring dielectric constants in the range of centimeters waves," *J. Appl. Phys.*, vol. 17, pp. 610–616, July 1946.
[2] M. Wind and Rapaport, Ed., *Handbook of Microwave Measurements*, vol. I, 2nd ed. New York: Wiley-Interscience, 1954–1955, pp. 6–35, 10–23.
[3] N. Draper and H. Smith, *Applied Regression Analysis*. New York: Wiley-Interscience, 1966, p. 275.
[4] J. Todd, Ed., *Survey of Numerical Analysis*. New York: McGraw-Hill, 1962, pp. 257–261.
[5] M. Rodríguez-Vidal and E. Martín, "Contribution to numerical methods for calculation of complex dielectric permittivities," *Electron. Lett.*, vol. 6, p. 510, Aug. 1970.
[6] T. W. Dakin and C. N. Works, "Microwave dielectric measurements," *J. Appl. Phys.*, vol. 18, pp. 789–796, Sept. 1947.
[7] M. Wind and Rapaport, Ed., *Handbook of Microwave Measurements*, vol. I, 2nd ed. New York: Wiley-Interscience, 1954–1955, pp. 10–29.

A Lumped-Element Circulator without Crossovers

R. H. KNERR, SENIOR MEMBER, IEEE

***Abstract*—It is proposed to construct a simple "crossoverless" lumped-element circulator, which can be made without sophisticated thin-film processing. The circulator can be described by a "delta connected" equivalent circuit. A simple capacitor arrangement can be used to influence the three eigenvalue phases of the circulator independently, thus permitting this circulator to be maximized systematically. A set of computer-generated eigenvalues gives insight into the behavior of the device under varying operating conditions. Preliminary measurements using a very simple pattern on a 0.650-in-diam ferrite substrate show a 20-dB bandwidth of 10 percent and an insertion loss < 1 dB (0.3 dB/min) at *L* band.**

Manuscript received May 21, 1973; revised December 13, 1973.
The author is with Bell Laboratories, Allentown, Pa. 18103.

INTRODUCTION

The construction of lumped-element circulators at higher frequencies [1]–[3] was made possible by using thin-film crossover techniques which, together with a new approach to broad banding, lead to a completely symmetrical broad-band lumped-element circulator. In order to eliminate processing problems at even higher frequencies, some studies were made to construct a small circulator which does not necessitate any complicated processing. Some preliminary *L* band results show that it is possible to build such a circulator. The theory proposed seems to be substantiated by eigenvalue measurements on a computerized network analyzer.

There exists a certain similarity with the ring circulator [3], [4]. However, the ring circulator uses three delta connected nonreciprocal phase shifters and the devices realized are significantly larger and more complicated than the present device.

THEORY

A lumped-element circulator with its *Y*-connected equivalent circuit shown schematically in Fig. 1 can be represented by an impedance matrix of the general form

$$\begin{bmatrix} V_1 \\ V_2 \\ V_3 \end{bmatrix} = \begin{bmatrix} \alpha & \beta & \gamma \\ \gamma & \alpha & \beta \\ \beta & \gamma & \alpha \end{bmatrix} \begin{bmatrix} I_1 \\ I_2 \\ I_3 \end{bmatrix} \quad \text{or} \quad [V] = [Z_1][I]$$

or in admittance form:

$$[I] = [Z_1]^{-1}[V], \qquad \text{for } [Z_1]^{-1} = \begin{bmatrix} a & b & c \\ c & a & b \\ b & c & a \end{bmatrix} \tag{1}$$

where, in the lossless case,

$$\text{Re } (\alpha) = 0$$
$$\beta = -\gamma^* \tag{2}$$

γ^* being the complex conjugate of γ.

Y and *Z* matrices have been chosen for the analysis because they can be easily related to the equivalent circuit.

In the special case of Fig. 1,

$$\alpha = \omega G(j\mu)$$
$$\beta = \omega G\left(-\frac{j}{2}\mu - \frac{k}{2}\sqrt{3}\right)$$
$$\gamma = \omega G\left(-\frac{j}{2}\mu + \frac{k}{2}\sqrt{3}\right) \tag{3}$$

where G is a geometry factor [1], [6] which determines the inductance used in the equivalent circuits, and μ and k are the elements of the Polder tensor:

$$\mu_{ik} = \mu_0 \begin{bmatrix} \mu & -jk & 0 \\ jk & \mu & 0 \\ 0 & 0 & 1 \end{bmatrix}. \tag{4}$$

In the case where losses are taken into account, μ and k become complex numbers which depend on frequency, applied magnetic field, and material parameters. It can be shown [6] that the matrix equation (1), which is valid for the *Y*-connected three port, is also valid for a Δ-connected one if the notation in Fig. 2 is used, i.e., *Y* "line" currents (I) become Δ "branch" currents (I). Since we are interested in terminal quantities, the matrix equation

$$[I] = [Z_1]^{-1}[V] \tag{5}$$

has to be transformed into

$$[i] = [Y_1][u] \tag{6}$$

using the notation in Fig. 2, where [6]

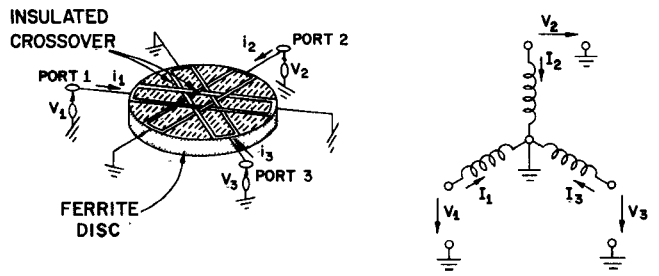

Fig. 1. (a) Y-connected lumped-element circulator junction. (b) Its approximate equivalent circuit.

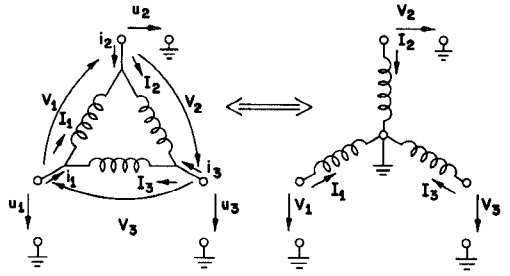

Fig. 2. Δ–Y equivalence.

$$[Y_1] = \begin{bmatrix} 2a-b-c & 2b-a-c & 2c-a-b \\ 2c-a-b & 2a-b-c & 2b-a-c \\ 2b-a-c & 2c-a-b & 2a-b-c \end{bmatrix} \tag{7}$$

α, β, and γ being defined in (1) and (3). The equation describes then the symmetrical Δ-connected three port in Fig. 2. For

$$\begin{aligned} A &= 2a-b-c \\ B &= 2b-a-c \\ C &= 2c-a-b \end{aligned} \tag{8}$$

(7) becomes

$$[Y_1] = \begin{bmatrix} A & B & C \\ C & A & B \\ B & C & A \end{bmatrix} \tag{9}$$

and is of the skew Hermitian type as the matrix in (1). For this three port to become an ideal circulator it has to satisfy Carlin's theorem [7] and

$$\begin{aligned} \text{Re}\,(A) &= 0 \\ B &= -C^* \end{aligned} \tag{10}$$

i.e., it has to represent a lossless three port. The matrix can satisfy both conditions and will be used to computer-generate scattering parameter eigenvalue curves.

Assume the circulator junction shown in Fig. 3(a) by three nonreciprocally coupled Δ-connected coils is excited by three voltages (in phase excitations):

$$\begin{bmatrix} u_1 \\ u_2 \\ u_3 \end{bmatrix} = \begin{bmatrix} 1 \\ 1 \\ 1 \end{bmatrix}. \tag{11}$$

The three voltages are in phase, and therefore the three terminals are at equal potentials, which in turn implies that the three coils appear to have zero impedance for the in-phase excitation.

If two sets of voltages (rotating excitations) of the form

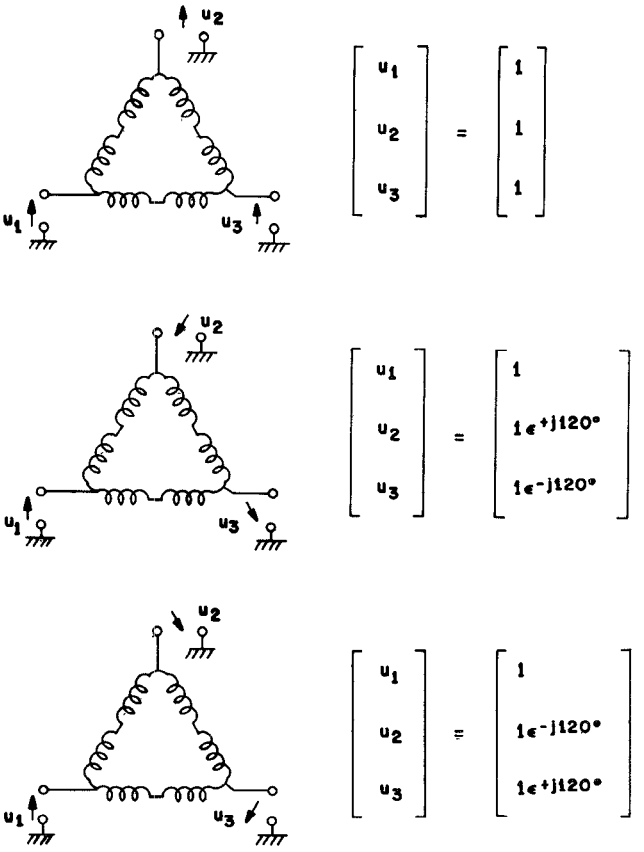

Fig. 3. Eigenexcitations of Δ circulator.

$$\begin{bmatrix} u_1 \\ u_2 \\ u_3 \end{bmatrix} = \begin{bmatrix} 1 & & \\ 1 & \epsilon^{+j120^\circ} & \\ 1 & \epsilon^{-j120^\circ} & \end{bmatrix}$$

$$\begin{bmatrix} u_1 \\ u_2 \\ u_3 \end{bmatrix} = \begin{bmatrix} 1 & & \\ 1 & \epsilon^{-j120^\circ} & \\ 1 & \epsilon^{+j120^\circ} & \end{bmatrix} \tag{12}$$

are applied as in Fig. 3(b) and (c), the coils represent a finite reactance, and the addition of capacitors, for example, in series or parallel with the inductors, does not change the fact that the voltages "see" a finite impedance while the in-phase excitation still sees zero impedance. The capacitors (or any impedance) therefore influence the rotating values only. The addition of this impedance Z_s then, as indicated in Fig. 4, changes the matrix in (1) to $[Z_2]$ where

$$[Z_2] = \begin{bmatrix} (\alpha + Z_s) & \beta & \gamma \\ \gamma & (\alpha + Z_s) & \beta \\ \beta & \gamma & (\alpha + Z_s) \end{bmatrix} \tag{13}$$

and

$$[V] = [Z_2][I] \tag{14}$$

which can be transformed into an equation using terminal quantities

$$[i] = [Y_2][u] \tag{15}$$

by using the transformation in (7). Using a matrix formulation similar to the one used in [1], it can be shown that the scheme shown schematically in Fig. 5 can be used to influence the three eigenvalues individually. One way of influencing only the fields due to the in-phase excitation is indicated in Fig. 5, where it is evident that the currents from the different excitations add through the impedance Z_0. Since the currents due to the rotating excitations are 120° out of

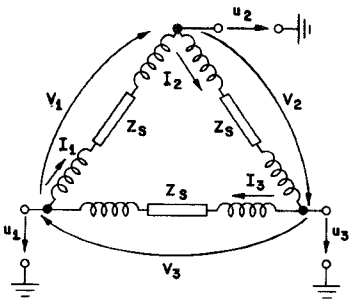

Fig. 4. Impedances (Z_S) which influence only the rotating eigenvalues.

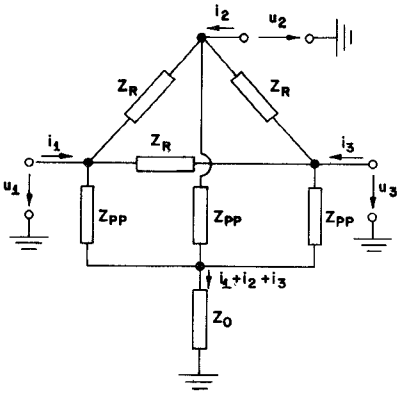

Fig. 5. Complete circuit for influencing the eigenexcitations individually.

phase, they cancel and only the currents induced by the in-phase excitations flows through Z_0. The impedance Z_{pp}, as the realization of the device will show, is always present, either intentionally or as a parasitic, and is seen by all three excitations.

COMPUTED RESULTS

A computer program was written to study the influence of the impedances Z_R, Z_{pp}, and Z_0 on the S-parameter eigenvalue phase and magnitude[1] as a function of frequency for different materials and resonators. Since it is difficult to achieve high-Q inductors at microwave frequencies, the impedances were, in the computer study as well as in practice, replaced by capacitors as indicated in Fig. 6. Since in the lossless case, an ideal circulator is defined by a 120° phase separation of the S-parameter eigenvalue phases [7], the maximization of the circulator performance is obtained by proper eigenvalue phase adjustment, as previously discussed [1]. Fig. 6 shows the S-parameter eigenvalue phase as a function of frequency for different values of C_s. As expected, the capacitor C_s influences only the eigenvalues due to the rotating excitations. A change of the value of the capacitance C_0 influences only the phase of the eigenvalue due to the in-phase excitation. It was mentioned before that the capacitors (Z_{pp}) influence all three eigenvalues which is indicated in Fig. 7(a) and (b) where C_s, for numerical reasons, has been chosen to be 100 pF which, for L-band frequencies, is a short circuit. The capacitors C_{pp} resonate in parallel with the nonreciprocally coupled inductors which translates into an eigenvalue phase change from +180 to −180°. The additional resonance in one eigenvalue phase occurs near the ferromagnetic resonance of the material, similar to the case described in more detail in [7]. The curves in Figs. 6 and 7 were all run at an internal biasing field of 150 Oe which corresponds to the so-called low-field operation of the circulator. Fig. 8 shows the eigenvalue phases and amplitudes at an internal field of 650 Oe (external field approximately 900 Oe) for different values of C_{pp}, the rest of the parameters remaining constant.

[1] For the derivation of the eigenvalue equations which can be easily applied to (13), see [1].

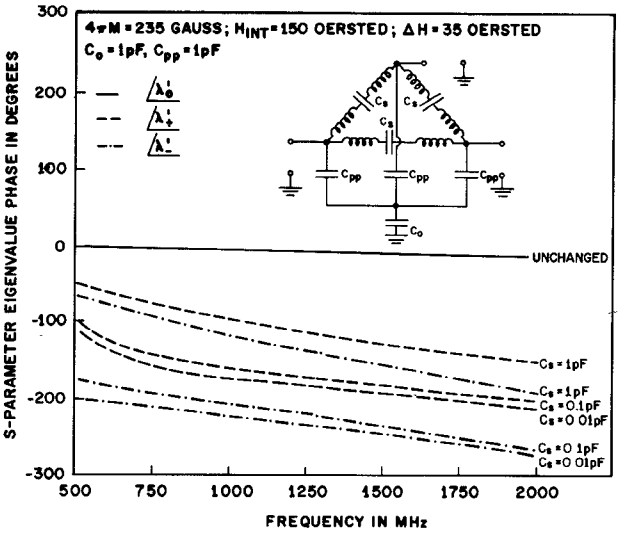

Fig. 6. Influence of the capacitors C_S on the eigenvalue phases.

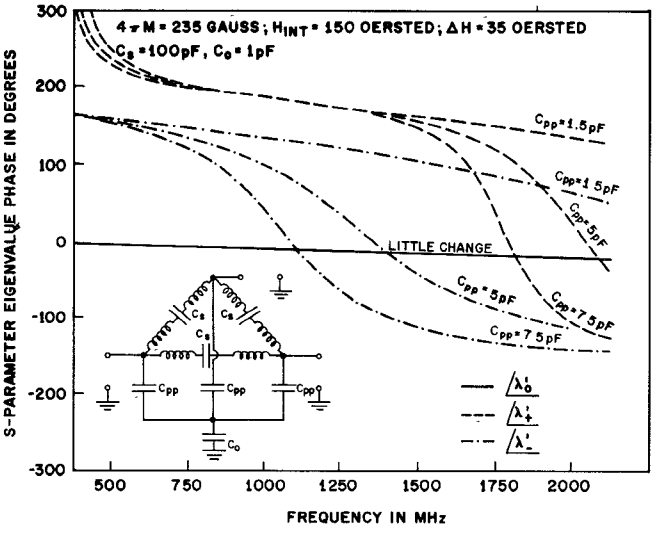

(a)

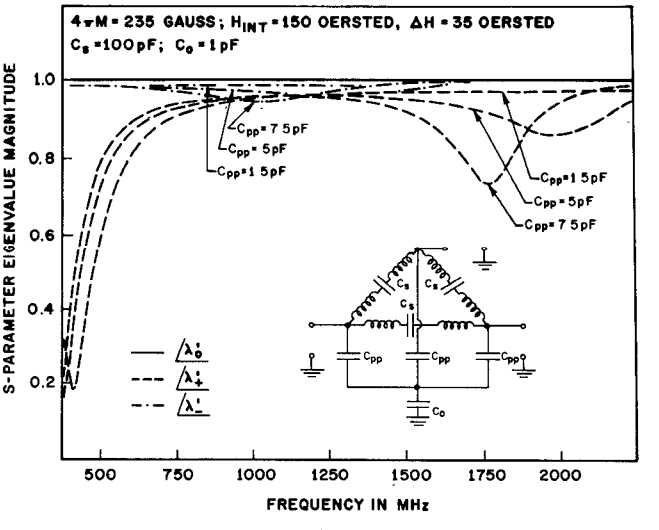

(b)

Fig. 7. (a) Influence of the capacitors C_{pp} on the eigenvalue phases. (b) Influence of the capacitors C_{pp} on the eigenvalue magnitude.

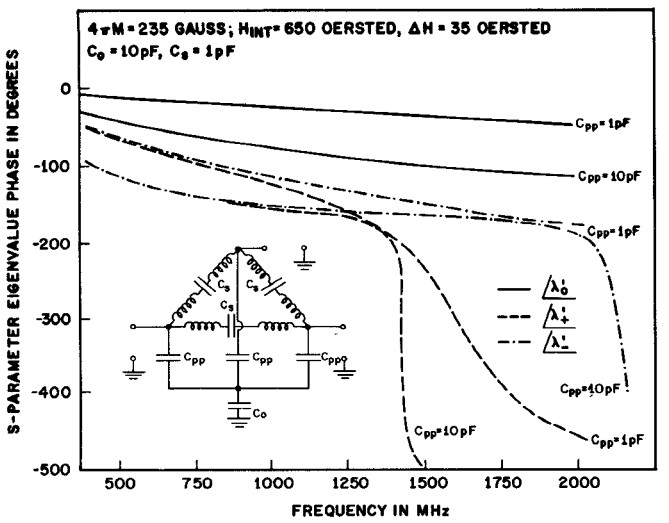

Fig. 8. Influence of capacitors C_{pp} on the eigenvalue phase as in Fig. 7 but for a higher internal field.

EXPERIMENTAL RESULTS

It should be kept in mind that the curves obtained by the computer simulation are a result of the matrix transformation described before. This is a purely mathematical transformation, and the generated curves verify that it is a valid one and that a structure of this type is theoretically capable of the same performance as a Y circulator. The theory naturally contains the assumptions of the Y theory which assumed 100-percent coupling between the inductors.

There are many possible structures implementing the Δ-connected equivalent circuit. Since the capacitors C_{pp} are always present[2] and influence all three eigenvalues it seems useful at this time to discard initially the series connected capacitors C_s and use C_{pp} and C_0 only for the eigenvalue phase adjustment. This results in the simple structure shown in Fig. 9. Circuits of this type have been built and successfully tested. Fig. 10 shows the measured eigenvalue phase for a structure similar to the one in Fig. 9 with a ferrite disk diameter of 0.650 in. As expected from the previous discussion, the eigenvalue phase exhibits a parallel resonance as indicated by the phase change from $+180$ to $-180°$, which is due to the resonance of the inductor L and the capacitor C_{pp} in Fig. 7. This performance follows qualitatively the computed results in Fig. 8, although the splitting is less than expected. Obviously, a further shaping of the in-phase eigenvalue phase in order to track the rotating eigenvalue phases over a larger frequency range would lead to an increase in bandwidth.[3] However, the device operates above resonances which implies less bandwidth potential. The slopes of the eigenvalue phases are steeper for above-resonance operation (Fig. 8) than for below-resonance operation (Fig. 7). Because of increased losses close to resonance, there is expected to be a greater insertion loss variation over the band. Fig. 11 shows the measured performance of such a circulator. The circulator operated above resonance at an applied field of about 1000 Oe (the fields in the eigenvalue plots are internal fields). The achieved performance of a 20-dB bandwidth of 10 percent and a minimum insertion loss of 0.3 dB in preliminary tests is sufficient for some applications and warrents further investigation of broad banding the device and exploration of the high frequency (i.e., size) limitations.

This type of circulator can be switched without changing the magnetic biasing field by changing the values of the capacitors C_s and C_0 or C_{pp} and C_0. This type of switching, which was described previously by the author [9], can conceivably be done by semiconductors.

[2] If C_{pp} is not added as in Fig. 9, there exists a significant parasitic capacitance between the pattern and the bottom metallization of the ferrite.

[3] The resonance of the in-phase eigenvalue is due to a resonance of C_0 with the uncoupled inductance of the circulator similar to the case explained in [8].

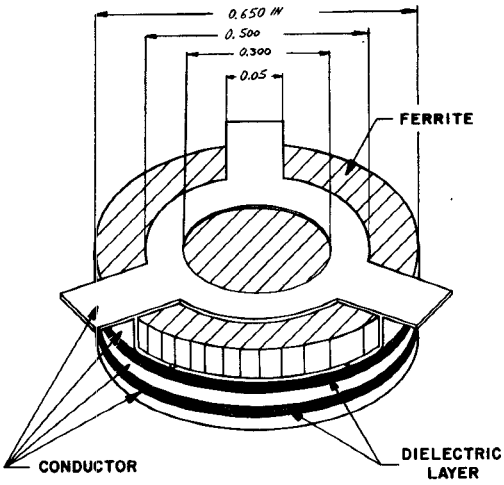

Fig. 9. Practical Δ circulator with additional capacitor at each port.

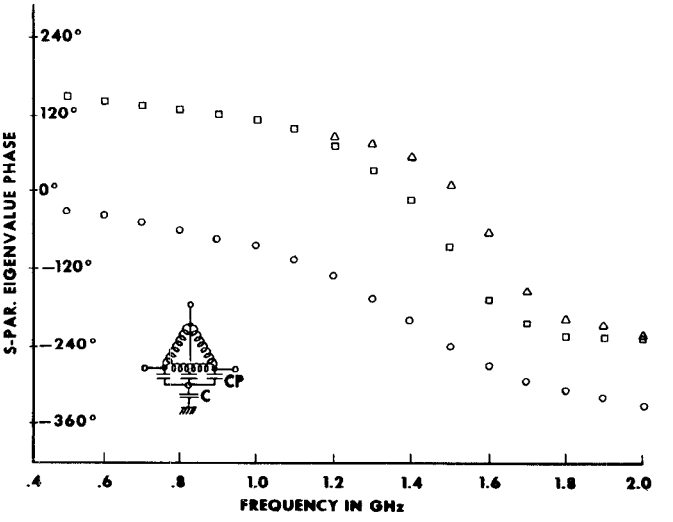

Fig. 10. Measured S-parameter eigenvalue phase as a function of frequency for experimental Δ circulator.

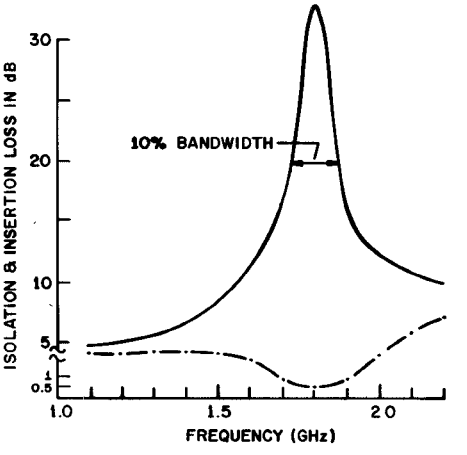

Fig. 11. Performance of experimental Δ circulator.

CONCLUSION

It has been shown that lumped-element circulators without crossovers can be easily built. Preliminary experimental results are encouraging, and it is expected that the 10-percent bandwidth reported can be increased moderately with additional effort. For large band-

widths, it would be advantageous to use below-resonance operation, and this should be further investigated.

Further work is required to realize experimentally the splitting obtained in the analysis and to evaluate the practical bandwidth and frequency limitations of this approach. It is anticipated that the crossoverless miniature lumped-element circulator will be particularly important at the higher microwave frequencies since the close tolerances and critical processing steps required in the crossover approach are avoided.

Computer generated and measured results are in qualitative agreement verifying the validity of extending the assumptions of the Y theory to the crossoverless device. It should be noted, however, that the analysis assumes an ideal 100-percent coupling between the inductors without considering where the coupling is physically obtained.

REFERENCES

[1] R. H. Knerr, C. E. Barnes, and F. Bosch, "A compact broad-band thin-film lumped-element L-band circulator," *IEEE Trans. Microwave Theory Tech. (1970 Symposium Issue)*, vol. MTT-18, pp. 1100–1108, Dec. 1970.

[2] R. H. Knerr, "A 4-GHz lumped-element circulator," *IEEE Trans. Microwave Theory Tech.*, vol. MTT-21, pp. 150–151, Mar. 1973.

[3] ——, "A microwave circulator that is smaller than a quarter," *Bell Lab. Rec.*, vol. 51, pp. 78–84, Mar. 1973.

[4] M. Grace and F. R. Abrams, "Three-port ring circulators," *Proc. IRE*, vol. 48, pp. 1497–1498, Aug. 1960.

[5] S. D. Ewing, Jr., and J. A. Weiss, "Ring circulator theory, design and performance," *IEEE Trans. Microwave Theory Tech.*, vol. MTT-15, pp. 623–628, Nov. 1967.

[6] E. Pivit, "Zirkulatoren Aus Konzentrierten Schaltelementen," *Telefunken J.*, vol. 38, p. 206, 1965.

[7] H. J. Carlin, "Principles of gyrator networks," in *Proc. Symp. Modern Advances in Microwave Techniques* (Polytech. Inst. Brooklyn, Brooklyn, N. Y.), Nov. 1954.

[8] R. H. Knerr, "An improvement equivalent circuit for the thin-film lumped-element circulator," *IEEE Trans. Microwave Theory Tech.*, vol. MTT-20, pp. 446–452, July 1972.

[9] ——, "A proposed lumped-element switching circulator principle," *IEEE Trans. Microwave Theory Tech.*, vol. MTT-20, pp. 396–401, June 1972.

Slot-Line Transitions

JEFFREY B. KNORR, MEMBER, IEEE

***Abstract*—Coax–slot and microstrip–slot transitions are discussed. Experimental VSWR and impedance data are presented and compared with values computed using equivalent circuits for these transitions. Thick-film chip terminations are also investigated.**

I. INTRODUCTION

Coax–slot and microstrip–slot transitions have been employed by a number of investigators and some experimental VSWR data have been reported [1], [2]. Equivalent circuits for these transitions have also been proposed [3]. However, no comprehensive comparison of experimental and theoretical performance has yet been published. The purpose of this short paper is to present the results of a study which was undertaken to compare the theoretical and experimental performance of these transitions.

II. COAX–SLOT TRANSITION

The coax–slot transition is shown in Fig. 1. It is constructed by placing miniature coaxial cable against the conducting surface and perpendicular to the slot at one end of the substrate. The outer

Manuscript received July 16, 1973; revised December 20, 1973.
The author is with the Department of Electrical Engineering, Naval Postgraduate School, Monterey, Calif. 93940.

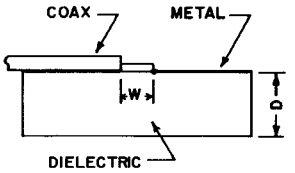

Fig. 1. Coax–slot transition.

conductor of the cable is electrically connected to one side of the slot with solder or epoxy and the center conductor is extended across the slot and bent down to meet the opposite edge where it is similarly secured. This is a rather easy transition to construct.

An approximate equivalent circuit for this geometrically complex transition has been obtained [3] through analysis of the simplified model shown in Fig. 2(a). The equivalent circuit is shown in Fig. 2(b) where

$$n = \frac{V(r)}{V_0} = \frac{\pi}{2} \mid k_c r H_1^{(1)}(k_c r) \mid \tag{1}$$

$$k_c = j\frac{2\pi}{\lambda'}\left(1 - \left\{\frac{\lambda'}{\lambda}\right\}^2\right)^{1/2}. \tag{2}$$

In these equations, $V(r)$ is the voltage at radius r, V_0 is the voltage directly across the slot, λ' is slot wavelength, and $H_1^{(1)}(k_c r)$ is a Hankel function. The coax–slot transition may be shunted by a short length of open-circuited slot line as well as by fringe capacitance at the open end of the slot. These effects are accounted for in the equivalent circuit by the lumped capacitance C. Typically, a millimeter of open-circuited 75-Ω slot line on a substrate with $\epsilon_r = 20$ has an input susceptance which is approximately equivalent to that of a 0.2-pF capacitor. L is the self-inductance of the semiloop of radius r.

Two coax–slot transitions were built and tested. The results were very similar for both and only one will be discussed in detail here. The transition was constructed with 50-Ω 0.141-in semirigid coaxial cable. This was coupled to a slot line etched from a 0.125-in-thick Custom Materials HI-K 707-20 ($\epsilon_r = 20$) substrate which was plated with 1 oz copper. Since the equivalent circuit predicts that the slot impedance will be transformed to a lower value, a slot impedance of about 75 Ω ($W/D = 0.55$) was selected. The slot was terminated at its other end with a 75-Ω thick-film chip resistor. The chip termination was obtained from EMC Technology, Inc., and consisted of a resistive film deposited on a 0.060- × 0.120- × 0.018-in alumina substrate. The chip was mounted upside down with epoxy thereby placing the resistive film directly across the slot. The termination has the same equivalent circuit as the transition, that of Fig. 2(b), with $n = 1$.

Experimental data for this transition were obtained using a microwave network analyzer. The reference plane was set at the transition and the data clearly indicated that the observed reflection coefficient was the vector sum of the reflection coefficients of the transition and the chip. The data were reduced accordingly using the theory of small reflections and the reflection coefficients of the two discontinuities were thus obtained. The method used did not account for losses due to radiation or attenuation in the slot, but these effects are believed to be very minor and any error is thus small.

The equivalent circuit of Fig. 2(b) was used to write equations for transition impedance and VSWR and these were then programmed. The values of slot impedance and slot wavelength required in the program were obtained from published curves [1]. Since there is no precise way to calculate L, C, or r, the program was used only for analysis in this study. The self-inductance L was measured using a TDR and found to be 0.61 nH so this value was used in all calculations. This left two undetermined parameters, C and r, and these were varied within reasonable limits to obtain agreement with experimental results.

The theoretical and experimental VSWR's of the transition are shown in Fig. 3. It can be seen that the experimental curve is in reasonable agreement with the theoretical curve for $C = 0$ pF. A radius $r = 0.1$ in was used in these calculations. This is about 50